
Since January 2020 Elsevier has created a COVID-19 resource centre with free information in English and Mandarin on the novel coronavirus COVID-19. The COVID-19 resource centre is hosted on Elsevier Connect, the company's public news and information website.

Veterinary Microbiology 253 (2021) 108955

Contents lists available at ScienceDirect

Veterinary Microbiology

journal homepage: www.elsevier.com/locate/vetmic

# A porcine epidemic diarrhea virus strain with distinct characteristics of four amino acid insertion in the COE region of spike protein

Zhaoyang Ji [1], Da Shi [1], Hongyan Shi, Xiaobo Wang, Jianfei Chen, Jianbo Liu, Dandan Ye, Zhaoyang Jing, Qiuge Liu, Qianjin Fan, Mingwei Li, Guangyi Cong, Jiyu zhang, Yuru Han, Xin Zhang *, Li Feng *

*State Key Laboratory of Veterinary Biotechnology, Harbin Veterinary Research Institute, Chinese Academy of Agricultural Sciences, Harbin, 150069, China*

ARTICLE INFO

*Keywords:*
Porcine epidemic diarrhea virus
Pathogenic
Alpha helix
Virus-Neutralization reactivity
Natural recombinant

ABSTRACT

In recent years, a novel, highly virulent variant of porcine epidemic diarrhea virus (PEDV) has emerged, causing substantial economic losses to the pork industry worldwide. In this study, a PEDV strain named LNsy was successfully isolated in China. Phylogenetic analysis based on the whole genome revealed that PEDV LNsy belonged to the G2 subtype. For the first time, a unique four amino acids (4-aa) insertion was identified in the COE region of the spike (S) protein (residues 499–640), resulting in an extra alpha helix in the spatial structure of the COE region. To determine changes in virus-neutralization (VN) antibody reactivity of the virus, polyclonal antibodies (PAbs) against the S protein of different subtypes were used in a VN test. Both PAbs against the S protein of the G1 and G2 subtype showed reduced VN reactivity to PEDV LNsy. Further, recombination analyses revealed that PEDV LNsy was the result of recombination between PEDV GDS13 and GDS46 strains at the genomic breakpoints (nt 17,959−20,594 in the alignment) in the ORF1b gene of the genomes. Pathological examination showed gross morphological pathological changes in the gut, including significant villus atrophy and shedding of the infected piglets. These results indicated that a 4-aa insertion in the COE region of the S protein may have partly altered the profiles of VN antibodies and thus it will be important to develop vaccine candidates to resist wild virus infection and to monitor the genetic diversity of PEDV.

## 1. Introduction

Coronaviruses (CoVs) are pathogens that can infect humans and animals and are divided into four genera: alpha-, beta-, gamma-, and delta-CoVs. PEDV belongs to the alpha-CoV group (Lin et al., 2016b). PEDV is an enveloped virus with a 28 kb single-stranded, positive-sense RNA genome. The genome of PEDV contains 5′-cap structures, a 3′-poly (A) tail, and six known open reading frames (ORFs): ORF1a/1b, spike (S), membrane (M), envelope (E), nucleocapsid (N), and an accessory protein gene, ORF3. PEDV is the main cause of global outbreaks of piglet diarrhea, which have caused great economic losses to the pig industry. PEDV was first reported in Europe in the 1970s and has since become common in other parts of the world (Choudhury et al., 2016).

In 2010, a highly virulent strain of PEDV appeared in China, and the mortality rate of newborn piglets was as high as 100 %, causing vast economic losses. In the United States, two types of PEDV strains have been identified based on the S gene: (1) the original highly virulent US PEDV (Stevenson et al., 2013), which is usually classified as the non-S INDEL PEDV; (2) the S INDEL PEDV, which has insertions and deletions in the N-terminal region of the S protein and results in reportedly milder disease in the field (Vlasova et al., 2014a; Wang et al., 2014). Phylogenetic analysis has shown that some S INDELS PEDV strains that have reported decreased virulence in the field (Vlasova et al., 2014a).

The S protein mediates entry of PEDV into host cells by binding the putative receptors aminopeptidase N and sialic acid (Li et al., 2016). The S protein is a type I glycoprotein composed of S1 and S2 subunits of the virus surface trimer (Li, 2016). S1 is involved in receptor binding, which involves the N-terminal domain (NTD) and C-terminal domain (CTD), both of which can serve as a receptor binding domain (Walls et al., 2016). The S2 subunit forms the stalk of the spike trimer, which is

* Corresponding authors at: State Key Laboratory of Veterinary Biotechnology, Harbin Veterinary Research Institute (HVRI), Chinese Academy of Agricultural Sciences, 678 Haping Road, Harbin, 150069, China.
*E-mail addresses:* zhangxin01@caas.cn (X. Zhang), fengli@caas.cn, fengli_h@163.com (L. Feng).
[1] These authors contributed equally to this work.

https://doi.org/10.1016/j.vetmic.2020.108955
Received 22 September 2020; Accepted 8 December 2020
Available online 13 December 2020
0378-1135/

involved in triggering fusion of the virus envelope and target cell membrane (Hulswit et al., 2016). The S protein is also the main envelope glycoprotein, which induces neutralizing antibody production (Wang et al., 2019). According to previous evolutionary analyses of S genes, PEDV is mainly divided into genome 1 (G1) and genome 2 (G2) clades and further divided into five subgroups: G1a, G1b, G1c, G2a, and G2b (Wang et al., 2016a). Mutations, deletions, and/or insertions in the S protein may alter its pathogenicity as well as virus-neutralization reactivity (Sun et al., 2018).

To study the biological characteristics of PEDV, further investigation of the diversity of PEDV is necessary. In this study, a 4-aa insertion was identified in the COE region of the S protein of a PEDV strain, resulting in the formation of an extra alpha helix in the spatial structure of the COE region. The cross VN test results revealed that polyclonal antibodies (PAbs) against S proteins of other PEDV strains have reduced neutralization reactivity to PEDV LNsy. These results will help in further analysis of the epidemic characteristics of PEDV. Furthermore, these results provide valuable information on PEDV recombination and evolution and will facilitate future investigations of the molecular pathogenesis of PEDV.

## 2. Materials and methods

### 2.1. Specimen collection, cell lines, and antibodies

In 2015, tissues from small intestines were harvested from pig farms suffering diarrhea in the Liaoning Province of China. The clinical symptoms were vomiting, yellow and watery diarrhea, rapid weight loss, and dehydration. Intestinal contents were collected from each infected piglet and mixed with phosphate-buffered saline (PBS; pH 7.2) at a ratio of 1:5. The suspension was then centrifuged at 6000×*g* for 15 min at 4 °C and filtered using a 0.22-μm filter. Vero E6 cells were cultured in Dulbecco's modified Eagle medium (DMEM, Gibco, USA) supplemented with 10 % fetal bovine serum (Gibco) and 100 U/mL penicillin-streptomycin (Sigma, USA), and incubated at 37 °C with 5% $CO_2$. PAbs against the S protein (Wang et al., 2016b), anti-PEDV S monoclonal antibody 6E5 (Li et al., 2019), and mouse anti-PEDV N monoclonal antibody 2G3 (Shi et al., 2017) were prepared in our laboratory.

### 2.2. Virus isolation

Small intestinal homogenates that tested positive by RT-PCR were prepared as 20 % (weight/volume) suspensions with DMEM. The suspensions were then vortexed and centrifuged at 5000 × g for 5 min and the supernatant was harvested. The supernatant was then filtered through a 0.2-μm filter (Millipore, Billerica, MA), and stored at −70 °C for virus isolation. Vero E6 cells were cultured in DMEM with 5% fetal bovine serum (FBS; Gibco) for approximately 2 days, and semi-confluent Vero E6 cells in a T25 flask were used for virus isolation. Before inoculation with intestine samples, cells were washed twice with PBS and 2 mL of the suspension collected in intestinal samples supplemented with 8 μg/mL trypsin (Gibco) was seeded into Vero E6 cells. Following incubation at 37 °C for 45 min, 5 mL DMEM containing 8 μg/mL trypsin was added to the cells and the inoculated cells were maintained at 37 °C under 5% $CO_2$ for 3–4 days, monitored daily for cytopathogenic effects (CPEs), and blindly propagated for several passages until CPEs were observed. The viral cultures were then subjected to freezing and thawing, and the cells and supernatants were mixed by pipetting and stored at −70 °C for further passages.

### 2.3. Indirect immunofluorescence assay (IFA)

Confluent monolayers of Vero E6 cells were infected with PEDV LNsy (multiplicity of infection of 1) for 24 h. The cells were then fixed with 4% paraformaldehyde at room temperature for 30 min, washed twice with PBS, and incubated with 0.1 % Triton X-100 at room temperature for 30 min. After two washes with PBS, the cells were blocked with 3% bovine serum albumin (BSA) for 2 h, washed three times with PBS, and incubated with mouse anti-PEDV N monoclonal antibody 2G3 for 2 h. Then, the cells were washed with PBS, Alexa Fluor®488-conjugated goat anti-mouse IgG (1:500 in BSA) was added, and the cells were incubated for 1 h at 37 °C in the dark. After washing with PBS, the cells were incubated with 4,6-diamidino-2-phenylindole (DAPI; 1:1000) for 30 min in the dark at room temperature. After washing three times with PBS, the cells were examined with an inverted fluorescence microscope (Life Technologies, USA).

### 2.4. Genomic sequencing of PEDV LNsy

Viral RNA was extracted from the supernatants using a RNA Extraction Kit (Tiangen, Beijing, China) according to the manufacturer's instructions. The viral RNA was then transcribed into cDNA as a template for PCR. The 16 pairs of primers for the complete genome sequencing of PEDV are listed in Supplementary Table S1. PCR products as shown in Supplementary Fig. 1 were purified and recovered using an AxyPrep™ DNA Gel Extraction Kit (Axygen Scientific, Inc., CA, USA) according to the manufacturer's instructions. The positive PCR products were cloned into pMD-18 T vector (TaKaRa, Dalian, China), The recombined plasmids were sequenced by TsingKe Biological Technology (Beijing, China).

### 2.5. Sequence analysis

The 16 overlapping fragments were spliced to obtain the complete genome sequence of PEDV LNsy. Multiple sequences of reference strains and PEDV LNsy were aligned using the Muscle method in MEGA 5 software. Phylogenetic trees based on the whole genome sequence and the S gene sequence were constructed using a maximum likelihood method with the Phylogeny Analysis function of MEGA software, and the bootstrap value was set as 1000 replicates. The aa sequence comparisons were analyzed using GeneDoc software. Recombination analysis was completed using RDP4 software. Methods including RDP, Bootscan, and SiScan were used. Likely parental isolates and recombination break points were detected with the default settings. The criterion for determining recombinations and breakpoints was a recombination score greater than 0.6.

### 2.6. Homology three-dimensional (3D) modeling

The spatial distribution of the partial S protein was analyzed in a 3D model using the SWISS-MODEL server. The S protein of PEDV strain LNsy, non-S INDEL strain PC22A (Lin et al., 2016a), and S INDEL strain USA Ohio126 2014 (Vlasova et al., 2014a) were modeled based on CV777 S protein. PyMOL software was used to represent structural figures.

### 2.7. VN test

The VN test was performed based on the method of fixed-virus diluted serum described by Reed and Muench. Briefly, Vero E6 cells were seeded into 96-well plates. Upon formation of confluent monolayers, the cells were washed three times with DMEM, and the PAbs against S protein were diluted two-fold starting at 1:25 with a final volume of 400 μL. Then, PEDV LNsy was diluted with DMEM supplemented with 10 μg/mL trypsin to a final volume of 400 μL containing 200 $TCID_{50}$. The PAbs and virus were mixed and incubated at 37 °C for 1 h. Finally, 0.1 mL of the mixture was added into the Vero E6 cells in 96-well plates. After 4 days, CPEs were observed using an inverted microscope. The VN titer, which is the highest dilution of serum that can protect 50 % of PEDV from infection, was calculated based on the Reed-Muench method.

### 2.8. Animal challenge

Six 3-day-old specific pathogen free piglets were randomly divided into two groups. Piglets in group A were challenged with $10^{5.0}$ $TCID_{50}$ of PEDV LNsy, while piglets in group B were challenged with DMEM as a control. Characteristics of the piglets in the two groups were observed daily. At 96 h post-infection, piglets were euthanized and examined for pathology. Intestine samples were fixed with 4% paraformaldehyde and examined for distribution of the virus by immunohistochemistry (IHC). During the experiment, the piglets were fed cow milk every 2 h, and lived in a comfortable environment. Throughout the experiment, animal care was conducted according to the guidelines of Animal Ethics Committee of HVRI (approval number: Heilongjiang-SYXK-2006−032).

### 2.9. Pathological examination and IHC staining

The intestinal samples were collected and immediately fixed with 4% paraformaldehyde in a 50 mL tube. The fixed intestinal samples were dehydrated, cleared in xylene, embedded in paraffin wax, sectioned, fixed on a glass slide, and stained with hematoxylin and eosin for observation using a standard microscope. The sections were then washed with PBS for 5 min, followed by antigen retrieval using 0.25 % trypsin in methanol and quenching of endogenous peroxidase activity with 3% $H_2O_2$ at room temperature for 30 min. The sections were again washed with PBS for 5 min, blocked with 5% goat serum, and incubated with monoclonal antibodies (mAbs) against S protein at a concentration of 2% at 37 °C for 1 h. Then, the samples were washed three times with

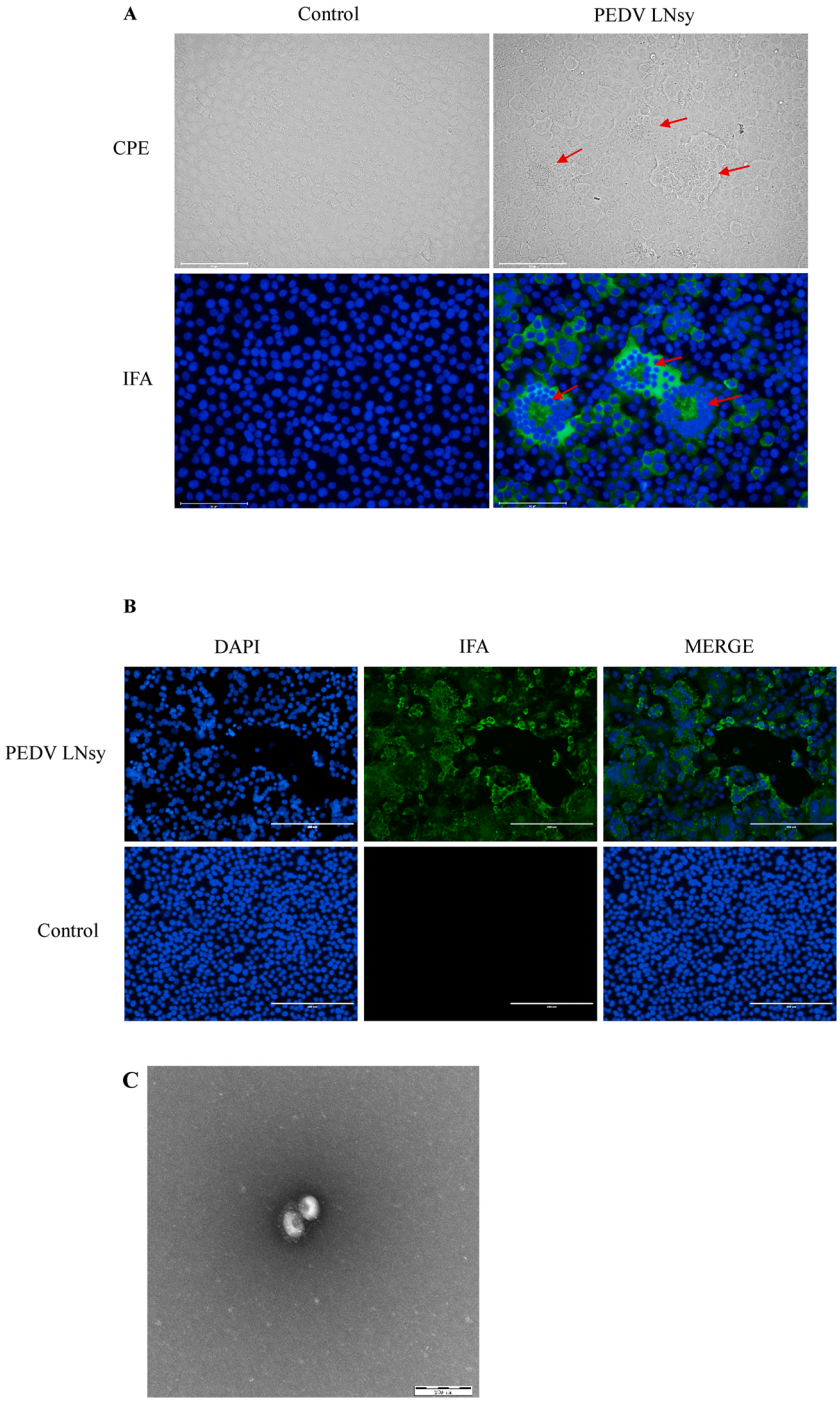


**Fig. 1.** Isolation and characterization of the PEDV LNsy strain. (A) Upper and lower panels show light and corresponding IFA images, respectively, of PEDV LNsy-infected Vero E6 cells using an inverted microscope. The infected cells show the formation of syncytia containing different numbers of nuclei (green for antigens, blue for nuclei). (B) IFA identification of PEDV LNsy. Infected cells were probed with anti-PEDV N mAb 2G3 and Alexa Fluor®488-conjugated goat anti-mouse IgG. (C) Electron microscopy observation of PEDV LNsy.

PBS for 5 min each, followed by the addition of horseradish peroxidase-labeled goat anti-mouse IgG secondary antibody and incubation at 37 °C for 1 h. Then, the samples were washed three times with PBS for 5 min each and incubated with DAB for 5−10 min. The samples were washed with water to stop staining, and coloration and counterstaining were performed with hematoxylin. After dehydration and mounting, the sections were observed under a microscope. Small intestinal samples were identified by location. In each of the three small intestinal sections, three perceived full-length villi and crypts were measured using a computerized image system (Image-Pro Plus software). The mean villous height to crypt depth ratios from each intestinal segment were used to determine villous atrophy.

### 2.10. Statistical analysis

We use one-way analysis of variance to determine the differences between groups. Data are expressed as mean ± standard error. All statistical analysis was performed with GraphPad Prism 5.0 software (GraphPad Software, Inc., La Jolla, CA, USA).

## 3. Results

### 3.1. Replication and cell adaptation of PEDV LNsy

To determine the causative agent of the diarrhea sampled at the Liaoning pig farm in China, total RNA isolated from the contents of small intestines was extracted and subjected to RT-PCR. The results showed that the samples were positive for PEDV (Supplementary Fig. 1). After passaging in the Vero E6 cell line, CPEs were observed, as evidenced by the rounding up and enlarging of cells, the formation of syncytia, and the detachment of the cells from the plate (Fig. 1A). The IFA showed specific fluorescence using mAbs against PEDV N in the PEDV LNsy-infected Vero E6 cells, but not in the negative control (Fig. 1B). When analyzed by electron microscopy, typical coronavirus-like particles with diameters of 100−120 nm were observed (Fig. 1C). The virus was named the PEDV strain LNsy. The $TCID_{50}$ of PEDV LNsy ($10^{6.0}$/mL) was measured using the Reed-Muench method.

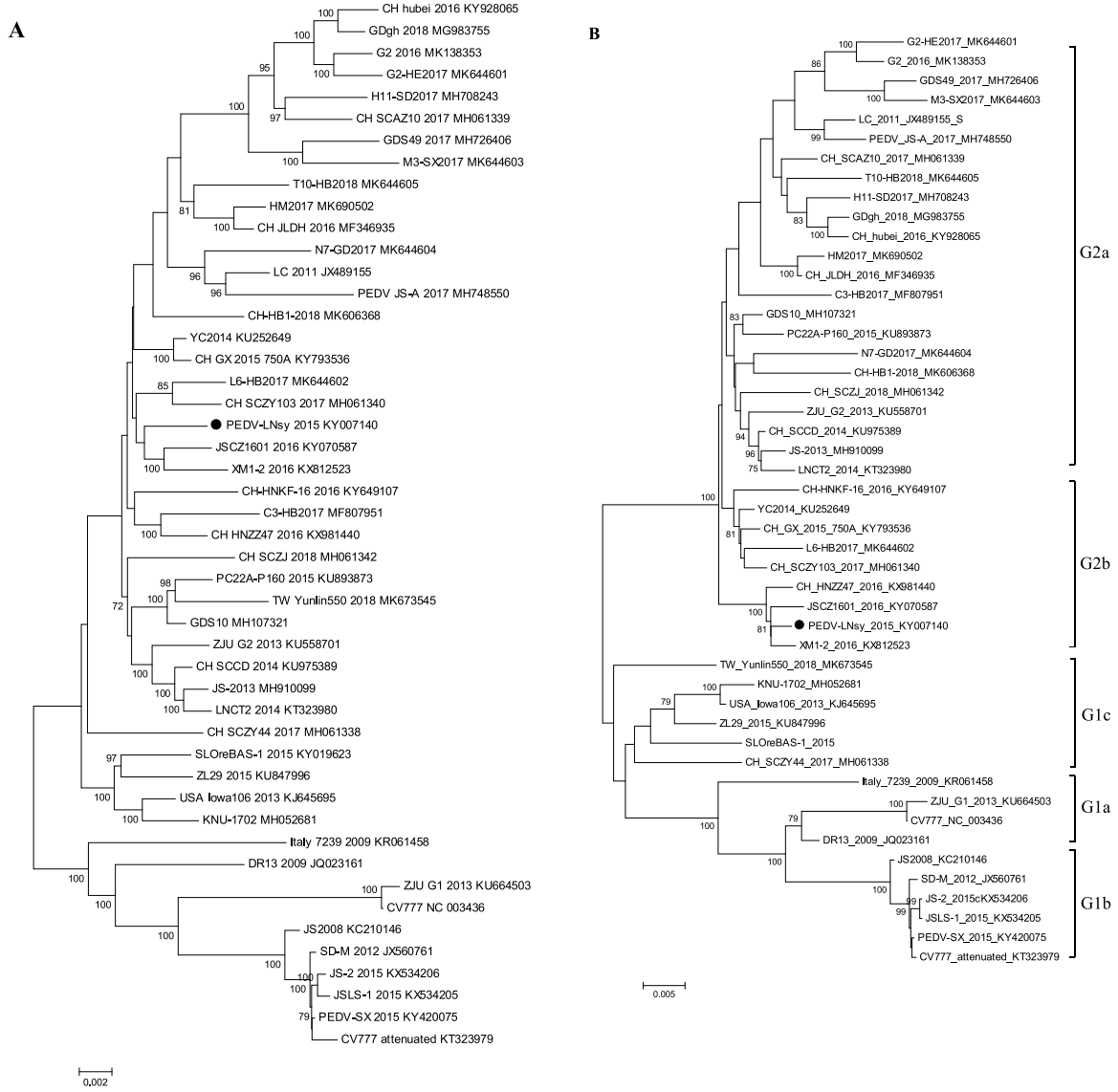


**Fig. 2.** Phylogenetic analysis of PEDV LNsy based on the complete genome and S sequence. Phylogenetic trees were constructed with MEGA 5.2 software using the construct/test neighbor-joining method (bootstrap method with 1000 replications). Bootstrap values > 70 % are shown. (A) Phylogenetic analysis of PEDV LNsy based on the complete genome. (B) Phylogenetic analysis of PEDV LNsy based on the S gene. The numbers at each branch represent the bootstrap values calculated by 1000 replicates. The scale bar indicates the nucleotide substitutions per site. The information on reference strains is provided in Supplementary Table S2.

### 3.2. Complete genome sequence of PEDV LNsy

The complete genome sequence of PEDV strain LNsy was deduced from overlapping cDNA fragments. The sequence was submitted to GenBank under accession number KY007140. A total of 28,050 nucleotides were determined for strain PEDV LNsy, encompassing ORFs 1a (nt 293−12,616), 1b (nt 12,616−20,637), S (nt 20,634−24,806), ORF3 (nt 24,806−25,480), E (nt 25,461−25,691), M (nt 25,699−26,379), and N (nt 26,391−27,716). Phylogenetic analysis showed that the PEDV strain LNsy was closely related to the G2 subgroup (Fig. 2A). Based on whole genome sequence alignments, the PEDV strain LNsy shares the most similarity with PEDV JSCZ (99.2 % nucleotide identity), while the vaccine strain CV777 and DR13 share 96.9 % and 97.6 % nucleotide identity, respectively (data not shown).

As an important virulence factor, the S gene is often used as a valuable molecular marker to determine genetic correlations between PEDV strains and to study the epidemiological situation. The nucleotide sequence of the PEDV LNsy S gene was 4173 nt in length, encoding a predicted S protein containing 1390 aa. A phylogenetic tree was constructed with selected PEDV S genes from GenBank (Supplementary Table S2) based on the nucleotide sequences of the S genes (Fig. 2B). The results showed that the PEDV LNsy strains identified in this study fell into the G2b subgroup.

### 3.3. The 4-aa insertion changed the spatial structure of the COE region

By comparing the aa sequences, we found that 4-aa (612QQSI615, number PEDV LNsy) were inserted in the COE region (Fig. 3A). The COE sequences (residues 499–640) of PEDV LNsy, PC22A and USA Ohio126 2014 were searched against the SWISS-MODEL template library, and the solution structure of the PEDV S protein (VP4) (SMTL id 6u7k.1) (Wrapp and McLellan, 2019) was selected for model construction. Compared with PEDV PC22A and USA Ohio126 2014, there was an insertion of 4-aa (Fig. 3B). The insertion of 4-aa resulted in an extra alpha helix in the spatial structure of PEDV LNsy.

We then analyzed VN antibody reactivity of PEDV strain LNsy. A cross VN test was performed, and the results showed that the average titer of $S_{CV777}$ PAb to neutralizing PEDV CV777, PEDV LNCT2, and PEDV LNsy was 375, 163, and 106, respectively. The average titer of $S_{LNCT2}$ PAb to neutralizing PEDV LNCT2, PEDV CV777 and PEDV LNsy was 390, 253, and 149, respectively. $S_{LNsy}$ PAb to neutralizing PEDV CV777, PEDV LNCT2, and PEDV LNsy was 106, 149, 289, respectively. Thus, both $S_{CV777}$ PAb and $S_{LNCT2}$ PAb, which belong to the G1 and G2 subtype, respectively, showed reduced VN antibody reactivity to the PEDV strain LNsy (Fig. 4). Therefore, compared with other PEDV strains, the 4-aa insertion not only changed the spatial structure of the S protein, but may also partly alter the profiles of VN antibodies. Intestinal lesions were apparent in the jejunum and mild lesions were observed in the duodenum and ileum. Villous atrophy was apparent in the small intestine, especially in the jejunum and ileum (Table 1)

### 3.4. Recombination of PEDV LNsy

To further analyze the association between PEDV LNsy and those of the existing isolates, a recombination examination and analysis was completed with RDP4 software (Martin et al., 2015). The results indicated that PEDV LNsy arose from recombination events between the GDS13 and GDS46 strains; breakpoints for potential recombination were found in the ORF1b region (nt 17,959−20,594 without gaps) (Fig. 5), and the major and minor parent strains of the recombination were GDS13 and GDS46, respectively (Fig. 5). These results suggest that PEDV LNsy was the result of a natural recombination event between GDS13 and GDS46.

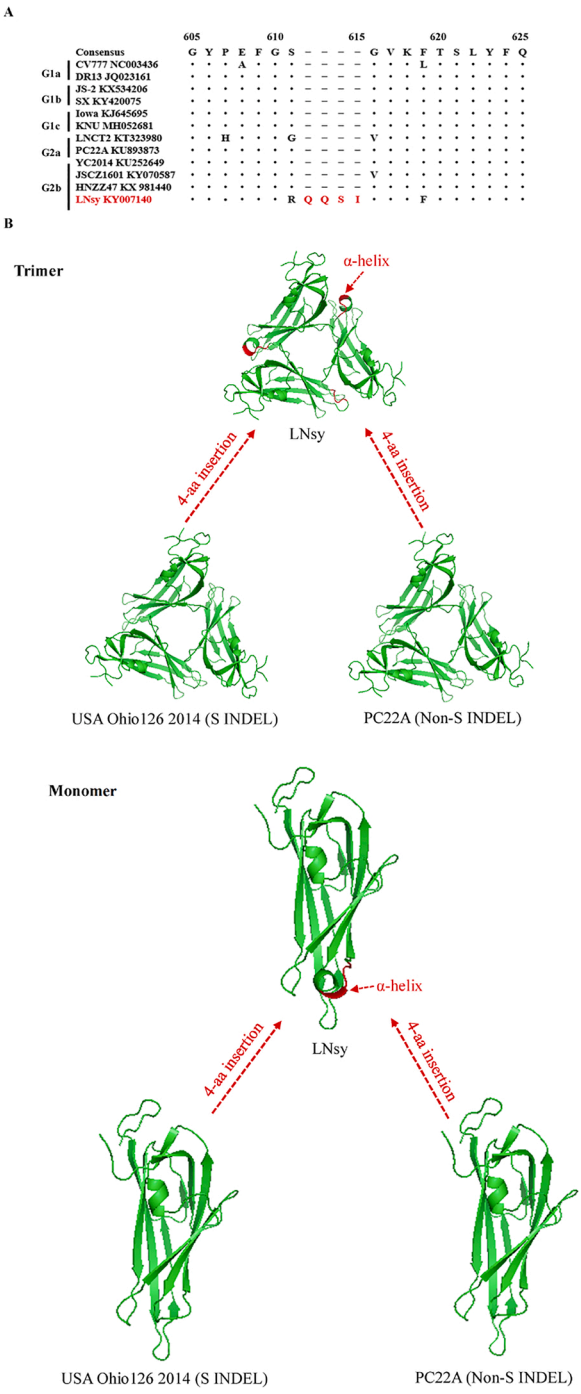


**Fig. 3.** Homology modeling of S protein with the 4-aa insertion in the COE region. (A) Sequence alignment of the S protein of different PEDV strains. Only PEDV LNsy shows the 4-aa insertion. (B) Effects of the 4-aa insertion in the COE region of the S protein on the spatial structure predicted by the SWISS-MODEL program. An extra alpha helix was present in the spatial structure of the COE region. The spatial structures of the COE region of the S protein were obtained from PEDV LNsy, USA Ohio126 2014, and PC22A. The red dotted line indicates the extra alpha helix.

### 3.5. Histopathological examination of PEDV LNsy-infected piglets

To evaluate the pathogenicity of PEDV LNsy, three piglets were orally inoculated with $10^{5.0}$ $TCID_{50}$ of PEDV LNsy and three control piglets were inoculated with DMEM. Vomiting and diarrhea were observed at 96 h post inoculation (hpi) of PEDV LNsy. None of the piglets inoculated with PEDV LNsy died over the course of the

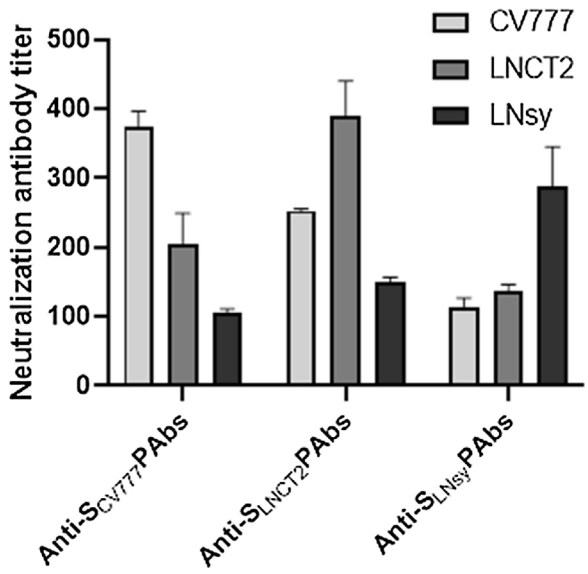


**Fig. 4.** Cross virus-neutralization (VN) between the S proteins of the two PEDV subtypes and anti-S PAbs. Reciprocals of PEDV neutralizing antibody titers were expressed as the dilution inhibiting PEDV infection by 50 %.

**Table 1**
Histology and immunohistochemistry analysis of intestines infected with PEDV strain LNsy.

| Group | VH:CD, mean(±SD)* | | | Antigen detection in the intestinal† |
|---|---|---|---|---|
| | Duodenum | Jejunum | Ileum | |
| Challenged | 1.7 (0.3) | 1.9 (0.5) | 1.7 (0.4) | + |
| Control | 3.3 (0.3) | 5.1 (0.9) | 3.4 (0.7) | − |

* VH: CD, ratio of villous height to crypt depth.
† Antigen detection by immunohistochemical staining:
+ epithelial cells showed staining;
− no epithelial cells showed staining.

experiment; all piglets were euthanized at 96 hpi. The control piglets did not show vomiting or diarrhea. Pathological changes were mainly observed in the jejunum and ileum. Fig. 6A shows villous atrophy, lymphoid aggregation of lymphocytes, and vacuolar degeneration of mucosal epithelial cells in the jejunum and ileum of PEDV LNsy-infected piglets, but not in the duodenum, colon, cecum, or rectum. IHC was used to demonstrate the location of PEDV LNsy using mAb 6E5 (specific for the S protein of PEDV). The S protein of PEDV LNsy was observed in the jejunum and ileum of piglets inoculated with PEDV LNsy (Fig. 6B). Labeling for PEDV LNsy was observed mainly in jejunal and ileal villi.

## 4. Discussion

PEDV has become one of the most common causes of viral diarrhea and has caused great harm to the pig industry around the world. Before October 2010 in China, PEDV infection was present in pig farms, but outbreaks were sporadic and regional, and no large-scale epidemic had been reported. After October 2010, a major outbreak with acute diarrhea as its clinical feature and piglet mortality as high as 80–100 % occurred in the southern provinces, causing high economic losses. Since 1994, inactivated or live attenuated PEDV CV777 strain vaccines have been developed. These inactivated and attenuated vaccines have been used extensively in the Chinese pig population, and have played an important role in the control of PEDV infections in China. At present, however, PEDV infection caused by mutant strains is prevalent in many pig farms in China. PEDV vaccines derived from classical strains cannot provide adequate immune protection against the currently prevalent strains (Ayudhya et al., 2012). This failure to provide complete protection may be caused by mutations in the virus, which pose a major challenge to the prevention and control of PED in China (Wang et al., 2016a). The monitoring and analysis of PEDV genes in the field will support an understanding of the trends in PEDV and aid in the development of more effective control measures.

The S gene is a common molecular marker in the study of genomic characteristics of PEDV strains. The CoV S protein binds to receptors and invades host cells, and thus, determines host range and cell tropism (Tortorici and Veesler, 2019). The cryoelectron microscopy structure of the PEDV S protein was previously identified in the prefusion conformation (Wrapp and McLellan, 2019). A new DØ region at the N terminus of S1 that arose from duplication of the NTD was identified in PEDV and may be more accessible to sialylated host cell surface proteins (Wrapp and McLellan, 2019). Previous studies have shown that the immunity induced by vaccines derived from CV777 is effective for the prevention of PED outbreaks caused by classical strains (Chen et al., 2019), and these vaccines have played an important role in the control of PEDV infections in China (Lin et al., 2016b). However, in recent years, with the continuous emergence of mutant PEDV strains, researchers have confirmed that the available commercial vaccines (G1) do not provide adequate immune protection against the currently prevalent strains (G2) (Lee, 2015). This phenomenon may be caused by virus mutations, which pose a major challenge to the prevention and treatment of PED in China.

Neutralizing antibody production is induced by the PEDV S protein, which contains several neutralizing epitopes: COE (residues 499–638) (Chang et al., 2002), GPRLQPY (2C10, residues 1368–1374) (Cruz et al.,

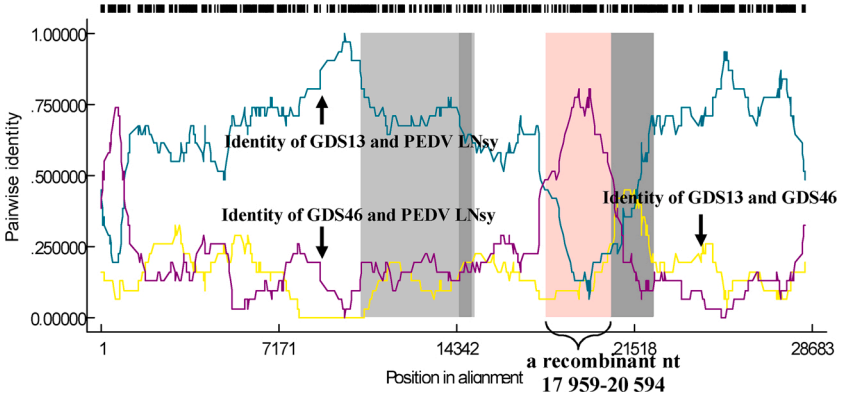


**Fig. 5.** Recombination analysis of PEDV LNsy with other PEDV strains. Genome recombination analysis of the PEDV LNsy strain. Recombination analysis was calculated with RDP4 software. Recombination breakpoints are shown with a pink background. The major and minor parent strains of the recombination were GDS13 and GDS46, respectively.

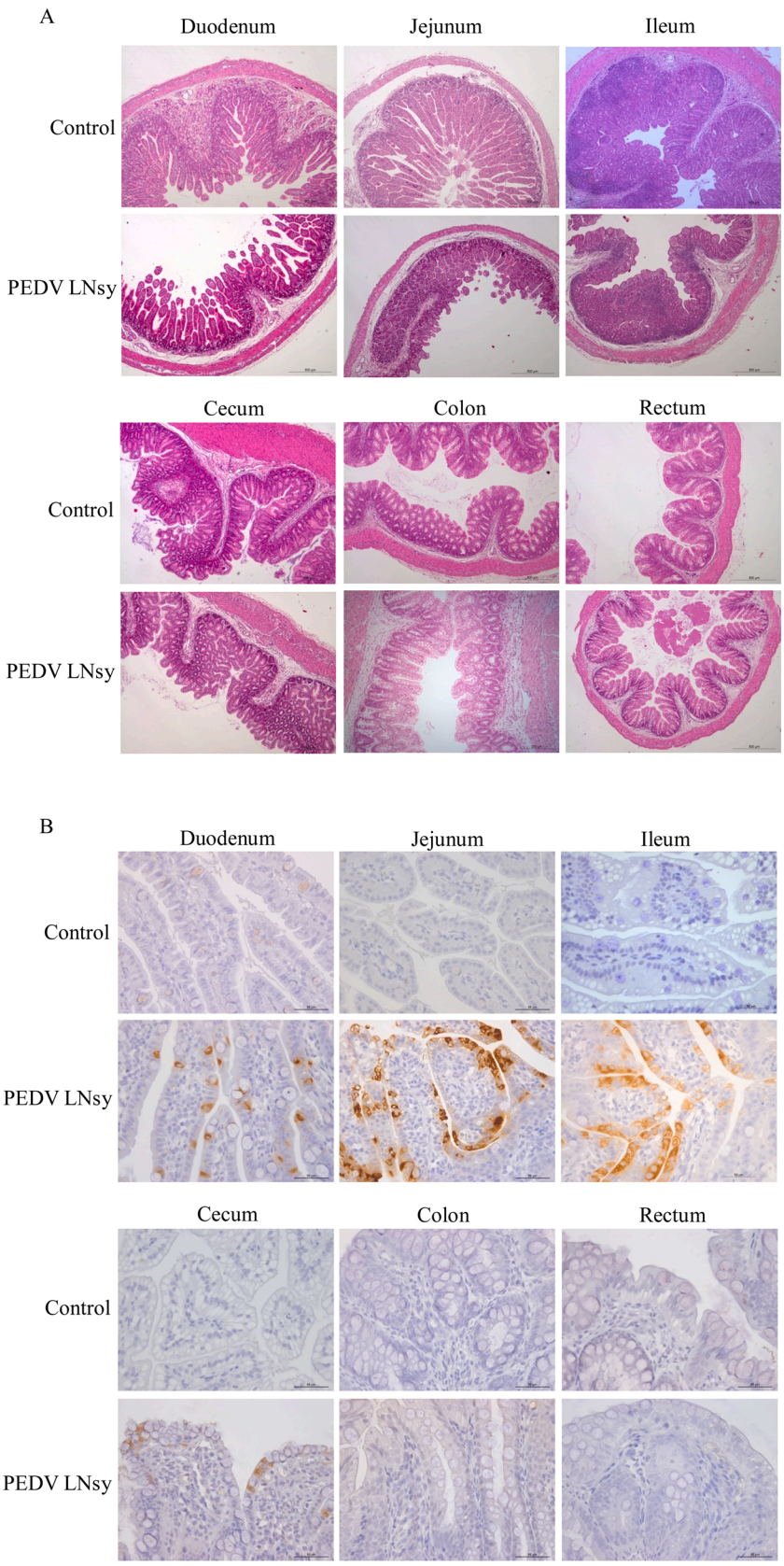


**Fig. 6.** Pathological changes and virus detection of the PEDV LNsy-inoculated piglets. (A) Pathological changes in tissues collected from the duodenum, jejunum, ileum, colon, cecum, and rectum of PEDV LNsy-inoculated piglets. Villus atrophy and capillary congestion occurred mainly in the small intestine. (B) IHC using the mAb 6E5 in the duodenum, jejunum, ileum, colon, cecum, and rectum of PEDV LNsy-inoculated piglets. Virus antigens were distributed mainly in the jejunum and ileum.

2008), S1D (residues 636–789) (Sun et al., 2007), S1° (residues 1–219), $S1^B$ (residues 510–640) (Li et al., 2017), P4B-1 (residues 575–639), E10E-1−10 (residues 435–485) (Chang et al., 2019), SS2 (residues 748–755), and SS6 (residues 764–771) (Sun et al., 2008). Mutations in the S protein, especially deletions and insertions, may change its antigenicity, pathogenicity, and neutralization characteristics (Suzuki et al., 2016). Thus, in the future, we will monitor changes in nucleotides and aa in the S region, which plays an important role in PEDV variation. Monitoring the neutralization epitopes of PEDV is helpful to understand the epidemic situation of PEDV. In this study, for the first time, a 4-aa insertion in the COE region of the S protein in PEDV was identified, resulting in an additional alpha helix in the spatial structure of the COE region. The VN test showed altered profiles of VN antibody reactivity of PEDV LNsy (Fig. 4). We speculate that these structural changes may affect the spatial conformations of the neutralizing epitopes of the S protein and the ability of the host to produce neutralizing antibodies. On the other hand, these changes may affect the binding affinity of neutralizing antibodies for the S protein, leading to a difference in cross-protection ability between different viruses. Meanwhile, because of the immune pressure of vaccines, aa substitutions in neutralizing epitopes may alter antibody epitope profiles, conferring the capacity for immune evasion in PEDV field strains (Sun et al., 2018). All these factors need to be further determined by future research.

In the present study, piglets developed mild diarrhea at 48−72 hpi, and no deaths occurred during the experiment. The pathogenicity of non-S INDELs PEDV strain PC22A resulted in diarrhea in piglets immediately at post challenge day (PCD) 1, and death occurred at PCD 2 (Langel et al., 2019). Although PEDV strain LNsy is pathogenic to piglets, disease severity was not consistent with non-S INDEL PEDV strain PC22A. A previous report showed that S INDELs and the associated single-nucleotide polymorphisms in the hypervariable S1 region of the S gene may be associated with decreased virulence (Vlasova et al., 2014b), indicating that PEDV strain LNsy might be an attenuated strain.

Recombination has been shown to be an important means of viral evolution and CoVs have high mutation rates due to recombination, resulting in changes in tissue tropism, transmission route, and host specificity. Gene recombination is a common phenomenon in CoVs (Forni et al., 2017) and has been reported previously in animal CoVs, such as TGEV (Zhang et al., 2017) and IBV (Ma et al., 2019). Recombination in PEDV is also a widespread phenomenon. Several reports have identified recombinant sequences (Supplementary Table S3) in the PEDV S gene (Qin et al., 2019), ORF1a (Jie et al., 2018), and ORF1b (Chen et al., 2017); recombination across multiple genes has also been shown (Jarvis et al., 2016). Among CoVs, homologous RNA recombination is a major factor underlying genetic evolution and diversity (Ntafis et al., 2011; Woo et al., 2009). Under field conditions, mixed infections are required to give rise to recombination events. There are many strains of PEDV in China, including classical, emerging, vaccine, and variant strains, providing increased opportunities for reorganization. In this study, breakpoints for potential recombination were found in the ORF1b gene, and these data will provide valuable information regarding PEDV recombination and evolution. The ongoing discovery of recombinant strains has indicated that PEDV infection in Chinese farms is becoming increasingly complex, suggesting that future studies of the genetic evolution of new local circulating PEDV strains in China will be necessary.

The PEDV strains identified in this study from Chinese pig farms in 2018 were clustered into the G2b subgroup. Compared with the Chinese vaccine strain, these Chinese PEDVs were genetically distinct and had multiple variations in neutralizing epitopes, suggesting that the development of novel vaccines based on these new PEDV variants may be necessary for controlling PEDV epidemics in China. Furthermore, in this study, a natural recombination event was observed in a Chinese PEDV strain, and the crossover point for potential recombination was found in the ORF1b gene. These results provide valuable information on CoV recombination and evolution and will facilitate future investigation of the molecular pathogenesis of PEDV.

## Data availability statement

All data generated or analyzed during this study are included in this article.

## Declaration of Competing Interest

The authors declare no conflict of interest with this research.

## Acknowledgement

This study was supported by The National Key Research and Development Program of China (2017YFD0500104 and 2017YFD0501603), Heilongjiang Science Foundation Project (C2018066) and Agricultural Science and Technology Innovation Program (CAAS-ZDRW202008).

## Appendix A. Supplementary data

Supplementary material related to this article can be found, in the online version, at doi:https://doi.org/10.1016/j.vetmic.2020.108955.

## References

Ayudhya, S.N., Assavacheep, P., Thanawongnuwech, R., 2012. One world–one health: the threat of emerging swine diseases. An Asian perspective. Transbound. Emerg. Dis. 59 (Suppl 1), 9–17. https://doi.org/10.1111/j.1865-1682.2011.01309.x.

Chang, S.H., Bae, J.L., Kang, T.J., Kim, J., Chung, G.H., Lim, C.W., Laude, H., Yang, M.S., Jang, Y.S., 2002. Identification of the epitope region capable of inducing neutralizing antibodies against the porcine epidemic diarrhea virus. Mol. Cells 14, 295–299.

Chang, C.Y., Cheng, I.C., Chang, Y.C., Tsai, P.S., Lai, S.Y., Huang, Y.L., Jeng, C.R., Pang, V.F., Chang, H.W., 2019. Identification of neutralizing monoclonal antibodies targeting novel conformational epitopes of the porcine epidemic diarrhoea virus spike protein. Sci. Rep. 9, 2529. https://doi.org/10.1038/s41598-019-39844-5.

Chen, N., Li, S., Zhou, R., Zhu, M., He, S., Ye, M., Huang, Y., Zhu, C., Xia, P., Zhu, J., 2017. Two novel porcine epidemic diarrhea virus (PEDV) recombinants from a natural recombinant and distinct subtypes of PEDV variants. Virus Res. 242, 90–95. https://doi.org/10.1016/j.virusres.2017.09.013.

Chen, P., Wang, K., Hou, Y., Li, H., Li, X., Yu, L., Jiang, Y., Gao, F., Tong, W., Yu, H., Yang, Z., Tong, G., Zhou, Y., 2019. Genetic evolution analysis and pathogenicity assessment of porcine epidemic diarrhea virus strains circulating in part of China during 2011-2017. Infect. Genet. Evol. 69, 153–165. https://doi.org/10.1016/j.meegid.2019.01.022.

Choudhury, B., Dastjerdi, A., Doyle, N., Frossard, J.P., Steinbach, F., 2016. From the field to the lab - an European view on the global spread of PEDV. Virus Res. 226, 40–49. https://doi.org/10.1016/j.virusres.2016.09.003.

Cruz, D.J., Kim, C.J., Shin, H.J., 2008. The GPRLQPY motif located at the carboxy-terminal of the spike protein induces antibodies that neutralize Porcine epidemic diarrhea virus. Virus Res. 132, 192–196. https://doi.org/10.1016/j.virusres.2007.10.015.

Forni, D., Cagliani, R., Clerici, M., Sironi, M., 2017. Molecular evolution of human coronavirus genomes. Trends Microbiol. 25, 35–48. https://doi.org/10.1016/j.tim.2016.09.001.

Hulswit, R.J., de Haan, C.A., Bosch, B.J., 2016. Coronavirus spike protein and tropism changes. Adv. Virus Res. 96, 29–57. https://doi.org/10.1016/bs.aivir.2016.08.004.

Jarvis, M.C., Lam, H.C., Zhang, Y., Wang, L., Hesse, R.A., Hause, B.M., Vlasova, A., Wang, Q., Zhang, J., Nelson, M.I., Murtaugh, M.P., Marthaler, D., 2016. Genomic and evolutionary inferences between American and global strains of porcine epidemic diarrhea virus. Prev. Vet. Med. 123, 175–184. https://doi.org/10.1016/j.prevetmed.2015.10.020.

Jie, T., Benqiang, L., Jinghua, C., Ying, S., Huili, L., 2018. Preparation and characterization of an attenuated porcine epidemic diarrhea virus strain by serial passaging. Arch. Virol. 163, 2997–3004. https://doi.org/10.1007/s00705-018-3968-6.

Langel, S.N., Paim, F.C., Alhamo, M.A., Buckley, A., Van Geelen, A., Lager, K.M., Vlasova, A.N., Saif, L.J., 2019. Stage of gestation at porcine epidemic diarrhea virus infection of pregnant swine impacts maternal immunity and lactogenic immune protection of neonatal suckling piglets. Front. Immunol. 10 https://doi.org/ARTN72710.3389/fimmu.2019.00727.

Lee, C., 2015. Porcine epidemic diarrhea virus: an emerging and re-emerging epizootic swine virus. Virol. J. 12, 193. https://doi.org/10.1186/s12985-015-0421-2.

Li, F., 2016. Structure, function, and evolution of coronavirus spike proteins. Annu. Rev. Virol. 3, 237–261. https://doi.org/10.1146/annurev-virology-110615-042301.

Li, W., van Kuppeveld, F.J.M., He, Q., Rottier, P.J.M., Bosch, B.J., 2016. Cellular entry of the porcine epidemic diarrhea virus. Virus Res. 226, 117–127. https://doi.org/10.1016/j.virusres.2016.05.031.

Li, C., Li, W., Lucio de Esesarte, E., Guo, H., van den Elzen, P., Aarts, E., van den Born, E., Rottier, P.J.M., Bosch, B.J., 2017. Cell attachment domains of the porcine epidemic diarrhea virus spike protein are key targets of neutralizing antibodies. J. Virol. 91 https://doi.org/10.1128/JVI.00273-17.

Li, L., Fu, F., Guo, S., Wang, H., He, X., Xue, M., Yin, L., Feng, L., Liu, P., 2019. Porcine Intestinal Enteroids: a New Model for Studying Enteric Coronavirus Porcine Epidemic Diarrhea Virus Infection and the Host Innate Response. J. Virol. 93 https://doi.org/10.1128/JVI.01682-18.

Lin, C.M., Saif, L.J., Marthaler, D., Wang, Q., 2016a. Evolution, antigenicity and pathogenicity of global porcine epidemic diarrhea virus strains. Virus Res. 226, 20–39. https://doi.org/10.1016/j.virusres.2016.05.023.

Lin, C.M., Saif, L.J., Marthaler, D., Wang, Q., 2016b. Evolution, antigenicity and pathogenicity of global porcine epidemic diarrhea virus strains. Virus Res. https://doi.org/10.1016/j.virusres.2016.05.023.

Ma, T., Xu, L., Ren, M., Shen, J., Han, Z., Sun, J., Zhao, Y., Liu, S., 2019. Novel genotype of infectious bronchitis virus isolated in China. Vet. Microbiol. 230, 178–186. https://doi.org/10.1016/j.vetmic.2019.01.020.

Martin, D.P., Murrell, B., Golden, M., Khoosal, A., Muhire, B., 2015. RDP4: detection and analysis of recombination patterns in virus genomes. Virus Evol. 1 https://doi.org/10.1093/ve/vev003 vev003.

Ntafis, V., Mari, V., Decaro, N., Papanastassopoulou, M., Papaioannou, N., Mpatziou, R., Buonavoglia, C., Xylouri, E., 2011. Isolation, tissue distribution and molecular characterization of two recombinant canine coronavirus strains. Vet. Microbiol. 151, 238–244.

Qin, S., Hu, C., Yang, D., Wu, J., Yue, H., Tang, C., Zhang, B., 2019. Emergence of porcine epidemic diarrhea viruses with the novel S genes in Tibetan pigs in the Qinghai-Tibetan plateau in China. Virus Res. 270, 197652. https://doi.org/10.1016/j.virusres.2019.197652.

Shi, D., Shi, H., Sun, D., Chen, J., Zhang, X., Wang, X., Zhang, J., Ji, Z., Liu, J., Cao, L., Zhu, X., Yuan, J., Dong, H., Chang, T., Liu, Y., Feng, L., 2017. Nucleocapsid interacts with NPM1 and protects it from proteolytic cleavage, enhancing cell survival, and is involved in PEDV growth. Sci. Rep. 7, 39700. https://doi.org/10.1038/srep39700.

Stevenson, G.W., Hoang, H., Schwartz, K.J., Burrough, E.R., Sun, D., Madson, D., Cooper, V.L., Pillatzki, A., Gauger, P., Schmitt, B.J., Koster, L.G., Killian, M.L., Yoon, K.J., 2013. Emergence of Porcine epidemic diarrhea virus in the United States: clinical signs, lesions, and viral genomic sequences. J. Vet. Diagn. Invest. 25, 649–654. https://doi.org/10.1177/1040638713501675.

Sun, D.B., Feng, L., Shi, H.Y., Chen, J.F., Liu, S.W., Chen, H.Y., Wang, Y.F., 2007. Spike protein region (aa 636789) of porcine epidemic diarrhea virus is essential for induction of neutralizing antibodies. Acta Virol. 51, 149–156.

Sun, D., Feng, L., Shi, H., Chen, J., Cui, X., Chen, H., Liu, S., Tong, Y., Wang, Y., Tong, G., 2008. Identification of two novel B cell epitopes on porcine epidemic diarrhea virus spike protein. Vet. Microbiol. 131, 73–81. https://doi.org/10.1016/j.vetmic.2008.02.022.

Sun, J., Li, Q., Shao, C., Ma, Y., He, H., Jiang, S., Zhou, Y., Wu, Y., Ba, S., Shi, L., Fang, W., Wang, X., Song, H., 2018. Isolation and characterization of Chinese porcine epidemic diarrhea virus with novel mutations and deletions in the S gene. Vet. Microbiol. 221, 81–89. https://doi.org/10.1016/j.vetmic.2018.05.021.

Suzuki, T., Shibahara, T., Yamaguchi, R., Nakade, K., Yamamoto, T., Miyazaki, A., Ohashi, S., 2016. Pig epidemic diarrhoea virus S gene variant with a large deletion non-lethal to colostrum-deprived newborn piglets. J. Gen. Virol. 97, 1823–1828. https://doi.org/10.1099/jgv.0.000513.

Tortorici, M.A., Veesler, D., 2019. Structural insights into coronavirus entry. Adv. Virus Res. 105, 93–116. https://doi.org/10.1016/bs.aivir.2019.08.002.

Vlasova, A.N., Marthaler, D., Wang, Q., Culhane, M.R., Rossow, K.D., Rovira, A., Collins, J., Saif, L.J., 2014a. Distinct characteristics and complex evolution of PEDV strains, North America, May 2013-February 2014. Emerg Infect Dis. 20, 1620–1628. https://doi.org/10.3201/eid2010.140491.

Vlasova, A.N., Marthaler, D., Wang, Q.H., Culhane, M.R., Rossow, K.D., Rovira, A., Collins, J., Saif, L.J., 2014b. Distinct characteristics and complex evolution of PEDV strains, North America, may 2013-February 2014. Emerg Infect Dis. 20, 1620–1628. https://doi.org/10.3201/eid2010.140491.

Walls, A.C., Tortorici, M.A., Bosch, B.J., Frenz, B., Rottier, P.J.M., DiMaio, F., Rey, F.A., Veesler, D., 2016. Cryo-electron microscopy structure of a coronavirus spike glycoprotein trimer. Nature. 531, 114–117. https://doi.org/10.1038/nature16988.

Wang, L., Byrum, B., Zhang, Y., 2014. New variant of porcine epidemic diarrhea virus, United States, 2014. Emerg Infect Dis. 20, 917–919. https://doi.org/10.3201/eid2005.140195.

Wang, D., Fang, L., Xiao, S., 2016a. Porcine epidemic diarrhea in China. Virus Res. 226, 7–13. https://doi.org/10.1016/j.virusres.2016.05.026.

Wang, X., Chen, J., Shi, D., Shi, H., Zhang, X., Yuan, J., Jiang, S., Feng, L., 2016b. Immunogenicity and antigenic relationships among spike proteins of porcine epidemic diarrhea virus subtypes G1 and G2. Arch. Virol. 161, 537–547. https://doi.org/10.1007/s00705-015-2694-6.

Wang, Q., Vlasova, A.N., Kenney, S.P., Saif, L.J., 2019. Emerging and re-emerging coronaviruses in pigs. Curr. Opin. Virol. 34, 39–49. https://doi.org/10.1016/j.coviro.2018.12.001.

Woo, P.C., Lau, S.K., Huang, Y., Yuen, K.Y., 2009. Coronavirus diversity, phylogeny and interspecies jumping. Exp. Biol. Med. 234, 1117–1127.

Wrapp, D., McLellan, J.S., 2019. The 3.1-Angstrom Cryo-electron Microscopy Structure of the Porcine Epidemic Diarrhea Virus Spike Protein in the Prefusion Conformation. J. Virol. 93 https://doi.org/10.1128/JVI.00923-19.

Zhang, X., Zhu, Y., Zhu, X., Shi, H., Chen, J., Shi, D., Yuan, J., Cao, L., Liu, J., Dong, H., Jing, Z., Zhang, J., Wang, X., Feng, Li*, 2017. Identification of a natural recombinant transmissible gastroenteritis virus between purdue and miller clusters in China. Emerg Microbes Infec. https://doi.org/10.1038/emi.2017.62.